Current Applied Science and Technology e-ISSN: 2586-9396

Curr. Appl. Sci. Technol. 2025, Vol. 25 (No. 4), e0263943

Research article

Removal of Textile Dyes from Wastewater: A Study of γ-Irradiation on Adsorption and Physicochemical Properties of Diatomaceous Earth

Khemmanich Khamenkit, Pattra Lertsarawut, Jirapa Maisomboon, Sasikarn Nuchdang, Dussadee Ratanaphra and Wilasinee Kingkam*

Nuclear Technology Research and Development Center, Thailand Institute of Nuclear Technology, Nakhon Nayok, 26120, Thailand

Received: 12 July 2024, Revised: 24 October 2024, Accepted: 31 October 2024, Published: 28 January 2025

Abstract

Textile industrial wastewater is an important contributor to water pollution. Thus, it is crucial to minimize contaminants in industrial waste before releasing it into the environment. Methylene blue (MB) is commonly found in textile industry wastewater and can present significant risks to human health and the environment. The purpose of this work was to use γ-irradiation to modify diatomaceous earth (DE) to eliminate MB from textile wastewater. The effects of different doses of γ-irradiation on diatomaceous earth adsorption capacity were investigated. The structure and properties of modified diatomaceous earth were characterized using scanning electron microscopy (SEM), Fourier transform infrared spectroscopy (FTIR), Braeuer–Emmett–Teller (BET) (for surface area), x-ray diffraction (XRD), and x-ray fluorescence (XRF). The adsorption isotherm and kinetics of samples were also investigated. The adsorption behavior of textile dyes on DE samples was carried out using a UV-Vis spectroscopy technique. Adsorption of the textile dyes onto modified DE was studied by batch adsorption techniques to determine the optimum conditions at a temperature of 30ºC. The factors of this experiment were contact time (30, 60, 90, 120, 150, and 180 min) with diffrent gamma radiation dose levels: 0 kGy (control), 5 kGy, 10 kGy, 20 kGy, and 30 kGy. The results showed that modified diatomaceous earth had a high adsorption capacity for the textile dye, with removal efficiencies ranging from 82-96% within 30 min. The maximum adsorption capacity of γ-irradiated DE was 14.9 mg g^{-1}. This indicates that γ-irradiation of DE may enhance the adsorption rate. It could be a cost-effective and environmentally friendly approach for treating wastewater polluted with textile dyes.

Keywords: adsorption; γ-radiation; methylene blue; diatomaceous earth

*Corresponding author: E-mail: wilasinee@tint.or.th
https://doi.org/10.55003/cast.2025.263943

1. Introduction

Nowadays, major environmental problems are brought on by water contamination. This causes a health risk for humans and other organisms that use the water, as well as a decrease in the amount of oxygen in the water, which impacts the sustainability of animal life because oxygen is required for aquatic plant photosynthesis (Lakshmi et al., 2018; Memon et al., 2020). Most of the toxins in the water are due to human activity, whether it be household wastewater from washing, cooking, and other activities, or industrial wastewater from various chemicals. The textile industries are significant water consumers, generating a substantial volume of effluents daily at various stages of textile processing (Thamaraiselvan & Noel, 2015; Nagaraju et al., 2016). Several kinds of hazardous compounds were found in textile wastewater, with an average daily discharge of 200 L/kg of fabric (Kant, 2012; Holkar et al., 2016). When released directly into the environment or water, some textile dyes have the potential to have negative, long-lasting consequences on ecosystems (Robinson et al., 2001). Therefore, it is crucial to remove these colors from industrial effluents before releasing them into the environment. Methylene blue (MB) is a cationic dye commonly employed in the textile industry due to its low cost and easy availability. Prolonged and high-dose exposure to MB may lead to vomiting, anemia, and hypertension. MB has the ability to generate a highly reactive singlet species known as singlet molecular oxygen. This species, particularly at higher concentrations, can cause damage to DNA structures and can even enter the food chain. Approximately 5% of this dye is used for coloring, while the remaining 95% is discarded as waste (Albadarin et al., 2017; Pathania et al., 2017; Rizqi & Purnomo, 2017).

In order to control and treat wastewater before releasing it into water sources, there is a need for pollution standards and the development of new technology. Although there are many methods for treating metal in industrial wastewater, one very common method is the sorbent adsorption method. It prompted numerous researchers to pay attention and attempt to develop inexpensive adsorbents to increase efficiency using various techniques. As an alternative to more expensive sorbents such as bentonite, cheaper alternatives such as waste sludge, maine, algae (*Ulva lactuca* and *Sargassum*), bagasse fly ash, and almond peel have been tried. Activated carbon has been considered a common adsorbent appropriate for removing numerous contaminants because of its high capacity and adaptability; however, the cost of this adsorbent occasionally restricts its broad use and makes it commercially undesirable (Crini et al., 2019). An excellent adsorbent should possess an appropriate amount of capacity together with a large surface area, exhibiting both thermal and chemical stability. It should be readily accessible, cheap, sustainable, and easily regenerated, while also demonstrating high selectivity for the target substances. Diatomaceous earth (DE) is a silica rock composed of the fossilized skeletal remains of single-celled aquatic algae called diatoms, with a rigid skeleton made of hydrated silica (opal). It has unique advantages and desirable properties, such as low density, high permeability, low thermal conductivity, high adsorption capacity, high porous with high specific surface area and low-cost material (Bessedik et al., 2002; He et al., 2018). As a result, DE should work well as the base of an adsorbent.

Several studies demonstrated that diatomaceous earth had a remarkable capacity to remove many different kinds of pollutants (Salman et al., 2016; Alkan et al., 2018; Ma et al., 2020) and even its waste was employed in the adsorption process. The adsorption capacity of this adsorbent can be improved through modification methods leading to an increase in its removal efficiency (Akafu et al., 2019). So far, improvement of the adsorption properties DE with gamma-irradiation has not yet been studied. The purpose of

this work was to use γ-irradiation on diatomaceous earth to improve its ability to eliminate MB from textile wastewater. The structure and properties of modified diatomaceous earth were investigated. Besides, the effects of different doses of γ-irradiation on diatomaceous earth adsorption capacity were studied to find the optimum doses of γ-irradiation for enhancing adsorption capacity and removal percentage. Additionally, the adsorption isotherms and kinetics were determined to assess the potential suitability of the adsorbent for future commercial applications.

2. Materials and Methods

2.1 Materials

Natural diatomaceous earth (DE) was collected from Mae Tha District, Lampang. MB (Figure 1) and acidic/basic solution using in this study were supplied from Merck, Germany. The chemical composition of the diatomite is given in Table 1. Nitric acid (HNO_3, 65%) used in this experiment was purchased from RCI Labscan, Ireland. All chemicals except diatomaceous earth were of reagent grade and used as received. Deionized water was used throughout this study.

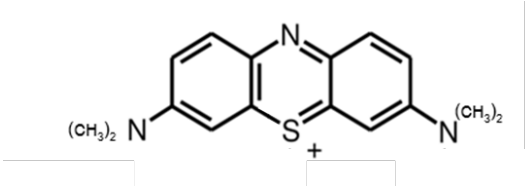

Figure 1. The structure of methylene blue

Table 1. Wavelength dispersive x-ray fluorescence (WDXRF) analysis of the DE and modified DE (concentrations in wt%)

Sample/ Element	Concentrations (%)				
	DE	DE 5 kGy	DE 10 kGy	DE 20 kGy	DE 30 kGy
Na_2O	0	0.52	0.8	0.48	0.37
MgO	0.37	0.32	0.3	0.31	0.34
Al_2O_3	10.15	9.96	9.98	9.99	10.08
SiO_2	82.28	82.53	82.1	82.39	82.27
K_2O	2.17	2.12	2.1	2.16	2.22
CaO	0.61	0.54	0.55	0.58	0.61
TiO_2	0.65	0.67	0.67	0.63	0.62
Fe_2O_3	3.34	3.29	3.31	3.38	3.44
Rb_2O	0.02	0.02	0.02	0.01	0.02
SrO	0.01	0.01	0.0095	0.01	0.01
ZrO_2	0.01	0.01	0.04	0.05	0.01

2.2 Diatomaceous earth preparation and irradiation

An acid-leaching stage was employed as a pretreatment method for the diatomite, aiming to eliminate trace amounts of impurity minerals prior to the extraction of silica. A 10 g sample of raw diatomaceous earth was subjected to leaching in a 100 mL solution of 2.2 M HNO_3 at a temperature of 60ºC for a duration of 3 h, with constant stirring at 750 rpm. The dispersion was then subjected to filtration, followed by multiple washes of the diatomite residue using deionized water. Subsequently, the residue was dried in an oven at a temperature of 110ºC overnight (Figure 2).

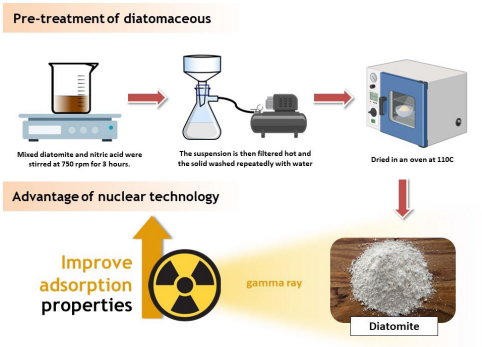

Figure 2. Process of diatomaceous earth preparation and gamma irradiation

The modified DE was produced by placing DE paste to various dosages of gamma irradiation ranging from 5 to 30 kGy at the Thailand Institute of Nuclear Technology in Nakhon Nayok, Thailand. The modified DE samples were designated as DE, DE 5 kGy, DE 10 kGy, DE 20 kGy and DE 30 kGy, following different conditions.

2.3 Characterization

The crystal structure and crystallite sizes of the DE was examined using X-ray diffraction (XRD) analysis. The XRD analysis was performed using a diffractometer (D8 Advance, Bruker AXS GmbH, Germany) with Cu Kα radiation. The diffractometer was operated at a current of 40 mA and a voltage of 40 kV. The analysis was conducted in the 2θ range of 10-90, with a scanning speed of 0.2° min^{-1}. The chemical composition of the DE was analyzed using X-ray fluorescence (XRF) technique. A scanning electron microscope (SEM-EDS, SU5000, Hitachi, Japan) was used to examine the surfaces and morphological features of the DE samples. Surface properties analysis was conducted utilizing a Micromeritics 3Flex apparatus equipped with N_2 adsorption and desorption capabilities. The Brunauer-Emett-Teller (BET) equation was employed to determine specific surface areas by analyzing adsorption isotherms and the BJH (Barrett-Joyner-Halenda) method was used to analyze the pore size distribution of mesoporous materials, particularly in the 2-50 nm range. It calculates pore sizes using nitrogen adsorption and desorption isotherms. The total pore volume is often estimated from the nitrogen adsorbed at a relative pressure (P/P_0) of 0.9, where P is the system pressure and P_0 is the saturation vapor pressure of nitrogen. Fourier transform infrared spectroscopy (FTIR) was conducted using a Perkin Elmer Spectrum Spotlight 300 instrument. The spectroscopy covered the range of 4000 to 400 cm^{-1} with a resolution of 4 cm^{-1}.

2.4 Batch adsorption experiments

The adsorption process was conducted using 100 mL of MB solution with a concentration of 250 mg/L and 1.5 g of diatomite, for both the raw and modified samples. The mixture was stirred for 30 min at room temperature in a beaker flask. Five milliliter samples were collected at various intervals over 180 min and transferred to separate cuvettes for settling. The time intervals were: 0, 30, 60, 90, 120, 150 and 180 min. This small sample volume ensured that the volume of MB solution remained constant throughout the experiment. The concentrations of MB were determined using a UV-Vis spectrophotometer at 665 nm. The following formula was employed to determine how much MB was adsorbed into each adsorbent sample (Mohseni-Bandpi et al., 2016; Touina et al., 2021):

$$\text{Adsorption efficiency} = \frac{C_0 - C_1}{C_0} \times 100 \quad (1)$$

$$qe = \frac{C_0 - C_e \times V}{M} \quad (2)$$

where q_e is the amount of dye adsorbed on the adsorbent at equilibrium (mg/g), C_0 and C_e are the initial and equilibrium of dye concentration (mg/L) in solution, respectively. V is the volume of solution (L), and M is the weight of adsorbent (g).

3. Results and Discussion

3.1 Adsorbents characterization

FE-SEM examination was performed to examine the surface morphology of both un-irradiated and γ-irradiated DE samples before the adsorption of MB. This analysis is depicted in Figure 3. The pretreatment sample was irregular, rough, and heterogeneous. The initial diatoms showed a cylindrical structure with a length of 15-20 μm and an internal pore diameter of about 1-2 μm. Smaller fragments having a tubular shape with a length of < 5 μm were also noticed in the Figure. The presence of macro-porosity and micron-scale features facilitates efficient reactant diffusion and physical separation processes. These structural characteristics contribute to an enhanced surface area, which improves the adsorption capacity and overall methylene blue (MB) removal efficiency (Jia et al., 2008). Furthermore, Figure 3(a-e) demonstrated that there was no change in the morphology of the DE. The presence of smaller fragments suggests potential for increased surface area and enhanced adsorption capabilities. Additionally, the consistent morphology after gamma irradiation indicated the stability of the diatomaceous earth structure under these conditions.

XRD patterns of diatomaceous earth, DE 5 kGy, DE 10 kGy, DE 20 kGy and DE 30 kGy are shown in Figure 4. The results identified that the raw diatomaceous earth was predominantly amorphous SiO_2 which is consistent with the quartz phases. The diffraction peaks at 20.95°, 26.75°, 36.54°, 39.46°, 42.44°, 50.13°, and, 59.95° corresponded to JCPDS no. 86-1630. The small diffraction peaks of 19.62° and 40.24° found were consistent with the montmorillonite phase with the chemical composition of sodium aluminum silicate hydroxide hydrate (JCPDS no. 12-0232). The experimental results showed that gamma irradiation had no significant effect on the crystal structures of the

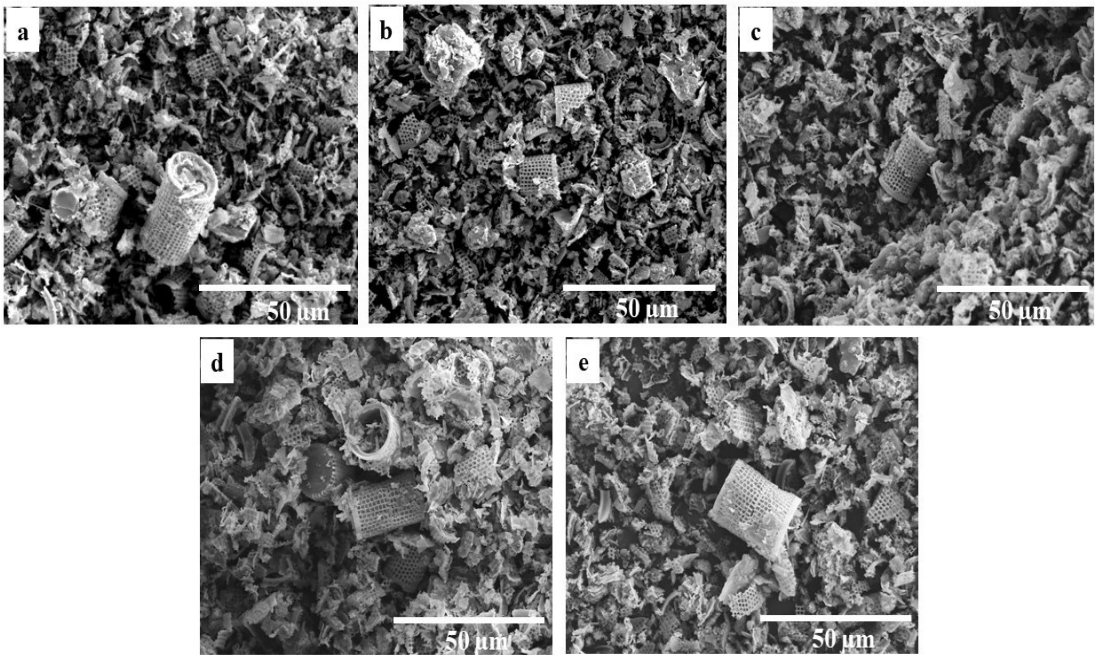

Figure 3. FE-SEM of DE with gamma radiation dose levels (a) DE, (b) DE 5 kGy, (c) DE 10 kGy, (d) DE 20 kGy and (e) DE 30 kGy

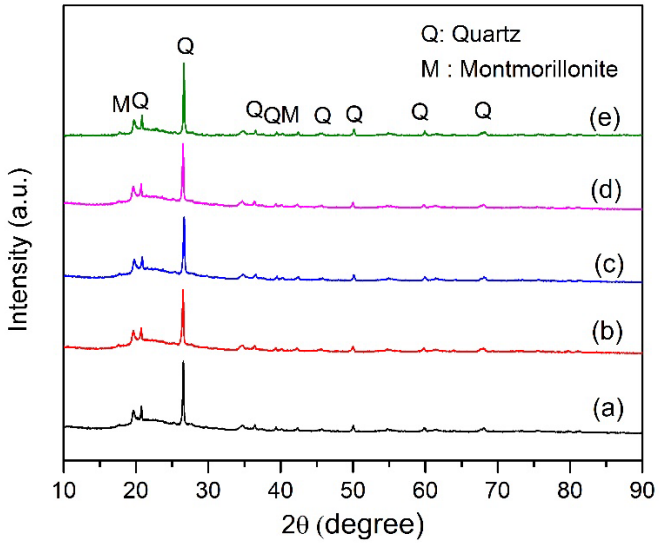

Figure 4. XRD patterns of DE with gamma radiation dose levels: (a) DE, (b) DE 5 kGy, (c) DE 10 kGy, (d) DE 20 kGy and (e) DE 30 kGy

modified diatomaceous earth samples. Similarly, the surface morphology of DE and modified DE exhibited either minimal changes or a slight reduction in surface features, indicating that gamma irradiation does not significantly alter the material's overall structure.

Table 1 provides a summary of the chemical composition of both DE and modified DE. The analysis shows that the primary constituent of natural diatomite was SiO_2, accounting for an average of 82%, followed by Al_2O_3, Fe_2O_3, and K_2O, respectively. Additionally, Na_2O was detected as a minor constituent in the modified DE, indicating that gamma irradiation induced significant changes in the chemical structure and composition of materials. When DE containing sodium silicates or sodium salts is exposed to gamma radiation, the radiation can break chemical bonds and cause decomposition or transformation of these compounds. For instance, gamma rays were shown to provide enough energy to break the Si-O or Na-O bonds in sodium silicate, leading to the release of Na_2O (Hsiao et.al, 2019; Rautiyal et.al, 2021). This was particularly noticeable in the DE sample irradiated at 10 kGy, where Na_2O was found in larger, more significant quantities than in other samples. The presence of Na_2O in the modified DE suggests that irradiation at 10 kGy may have led to the incorporation of sodium into the structure. This alteration could potentially impact the sorption properties and applications of the modified DE compared to natural DE.

FTIR approach was employed for confirming the existence of the functional groups in the DE before being used as a dye adsorbent. The spectra obtained from the FTIR analysis are presented in Figure 5. These results agreed with the corresponding XRD and XRF data. There were no significant variations in the exact positions of the primary characteristic bands. The characteristic peaks of DE were clearly indicated at 790 and 1070 cm^{-1} after reviewing the analysis data. Siloxane (–Si–O–Si–) stretching was found to be a broad and strong peak detected at 1070 cm^{-1} of DE 10 kGy, confirming the correctness of the compound (Galzerano et al., 2020). Other bands at 790 cm^{-1} were also characteristic of silica; the first one may be related to the stretching vibration of Al–O–Si (Vassileva et al., 2011). However, it is also possible to attribute it to the deformation of O-H or the presence of free silica and/or symmetric stretching of Si-OH (Khraisheh et al., 2004; Inchaurrondo et al., 2016). Variations in these peaks signify interactions between the dyes and silanol groups, which can be interpreted as adsorption on neutral sites (Rytwo et al., 2002). On the other hand, the second band is assigned to the bending vibrations of Si-O-Si (Yu et al., 2015). These results suggest that the compound analyzed is likely a form of silica with possible presence of Al-O-Si and Si-O-H. Further investigation may be needed to confirm the exact composition of the sample.

The possible mechanisms of dye adsorption onto the surface of diatomite are characterized by siloxane groups distributed throughout the silica matrix, as illustrated in Figure 6. The high energy ionizing radiation of gamma rays may lead to siloxane group (Si–O–Si–) bridges forming on the diatomite surface (Bakhsh, 2021). These bridges provided active sites for the adsorption of MB from aqueous solutions (Mohamed et al., 2019), indicating an electrostatic attraction between the positively charged MB and the negatively charged diatomite surface.

The specific surface area of the natural DE compared with modified DE decreased from 28.69 m^2/g to 22.51 m^2/g. The specific pore volume remained unchanged, and the average pore size also increased from 9.73 to 14.53 nm. By comparing the different samples of DE, it is obvious that DE's porous structure and physicochemical properties improved after gamma-irradiation surface modification as shown in Table 2. The average crystallite sizes of the DE, DE 5 kGy, DE 10 kGy, DE 20 kGy and DE 30 kGy were calculated as 11.91-58.16 nm using Debye–Scherrer's equation. The study also

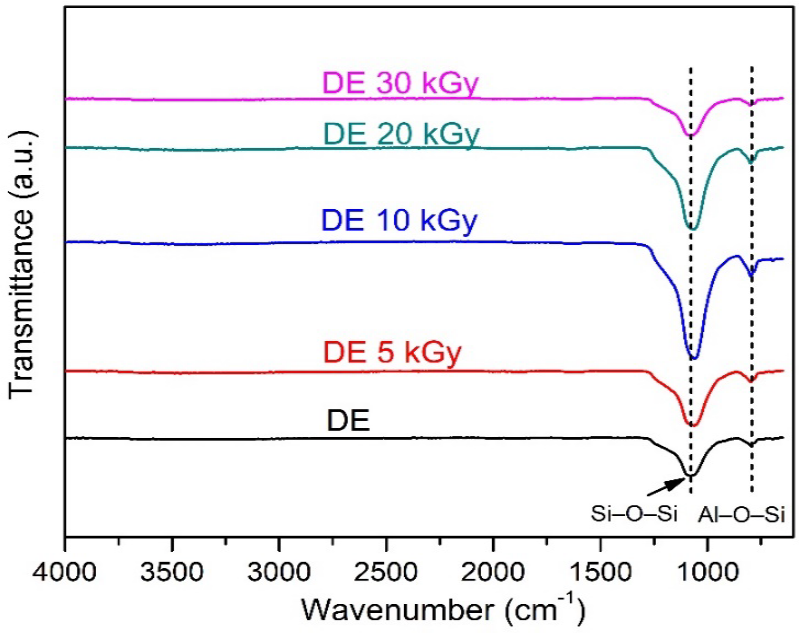

Figure 5. FT-IR spectra for the DE and modified DE

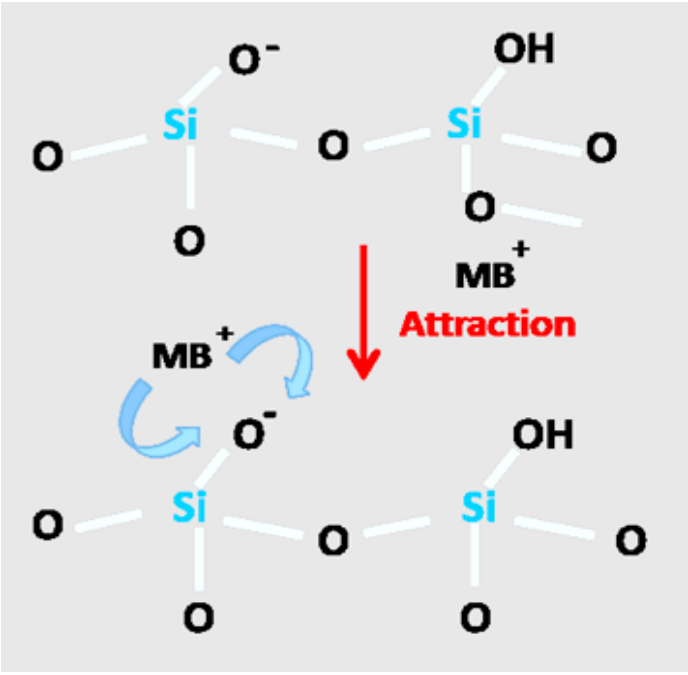

Figure 6. The possible adsorption mechanisms of MB onto DE surface

Table 2. Surface properties and crystallite size of natural DE and modified-DE

Catalyst	Specific Surface Area (m^2/g)	Pores Volume (cm^3/g)	Pore Size (nm)	Crystallite Size (nm)
DE	28.69	0.05	9.73	58.16
DE 5 kGy	25.34	0.03	10.86	20.11
DE 10 kGy	24.83	0.06	12.95	11.91
DE 20 kGy	26.81	0.06	12.17	17.27
DE 30 kGy	22.51	0.06	12.81	24.84

demonstrated that the average crystallite size of the modified DE increased with increasing dose of gamma radiation. The sorption capacities of the modified DE increase up to a certain radiation dose (10-20 kGy), but at 30 kGy the efficiency significantly drops. Similarly, when the radiation dose exceeded 10 kGy, the adsorption capacity gradually decreased, which could be due to a crosslinked reaction induced by gamma irradiation. It resulted in a more rigid, high crystallinity, and porosity decrease (Wang et al., 2019). This reduced porosity led to the decrease in the material's ability to adsorb synthetic wastewater.

3.2 Effect of γ -irradiation and contact time on the sorption properties

The experiment used gamma radiation to evaluate the adsorption of MB by modified DE. The adsorption trends of MB dye onto DE samples were studied across a time range of 30 to 180 min, as shown in Figure 7(a). It was found that the 10 kGy modified DE sample achieved equilibrium with MB. After 30 min, 97% of the MB dye was adsorbed. When the gamma radiation dose was increased to 30 kGy, there was no adsorption of MB dye at a concentration of 250 ppm. The adsorption capacity of MB on modified DE with gamma radiation doses of 0, 5.10, 20 and 30 kGy is shown in Figure 7(b). It was found that the DE and modified DE, except for DE30 kGy, had the ability to adsorb MB dye at 14.85, 14.87, 14.92 and 14.87 mg/g at the contact time of 180 min.

To determine the gamma irradiation effects on the sorption properties of DE, samples were treated at 0, 5, 10, 20 and 30 kGy. During the first 30 min, the adsorption percentages rose. However, from 60 to 180 min, the gains were sluggish, particularly for the all treated samples. After this time, no remarkable increase was witnessed, and the adsorption rate stayed steady. Thus, 90 min was chosen as the equilibrium time with 97% dye removal for DE, DE 5 kGy and 20 kGy, respectively. The adsorption equilibrium time for DE 10 kGy was established within 30 min, resulting in a quick removal of approximately 97%, as shown in Figure 8. This was because adsorbing gamma photons from the Co-60 onto DE would result primarily in Compton scattering and the formation of irradiation products due to water radiolysis (Daniels & Puri, 1986; Spinks & Woods, 1990). Compton scattering generates energetic dispersed electrons that are expected to shift mobile cations, and to some degree, framework atoms from their initial positions. This implies that the Na^+ ions, as indicated in Table 2 of the XRF data, together with other positively charged ions that were initially bound to the active sites of DE, may be neutralized by the incoming

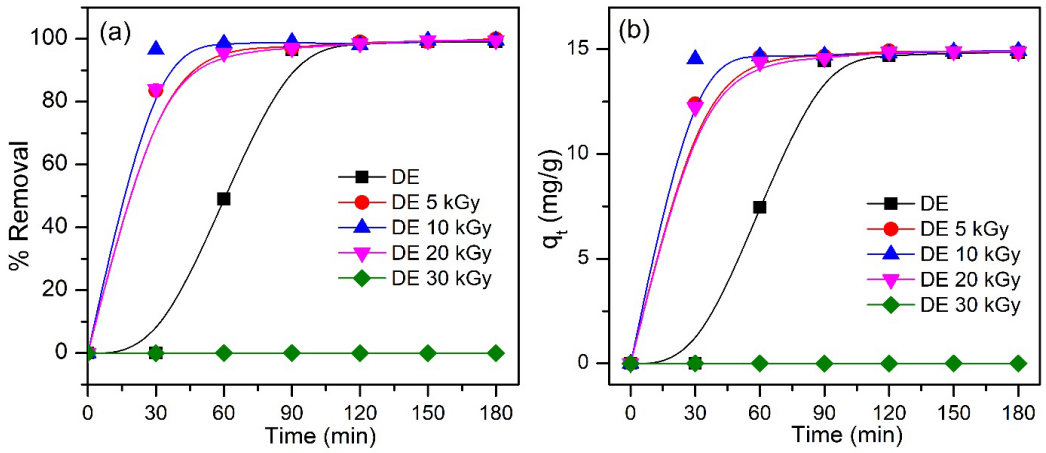

Figure 7. Adsorption of MB by DE and modified DE (a) % removal and (b) adsorption capacity vs. contact time

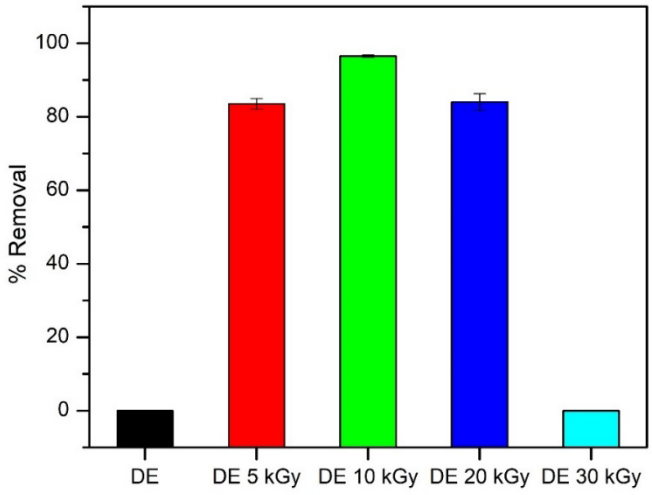

Figure 8. Effects of γ-irradiation on adsorption efficiency of DE and modified DE at 30 min

electrons. This electron transfer process could potentially lead to the reduction of Na^+ ions and other positively charged ions, resulting in a neutralization of the active sites on DE. Overall, this mechanism may play a crucial role in the removal of contaminants from water. As a result, these ions can get detached from the modified DE surface, causing the surface to acquire a higher negative charge. This results in a fast adsorption rate due to electrostatic attraction between the positively charged MB and the negatively charged diatomite surface. Moreover, these phenomena are especially likely to occur with gamma irradiation to DE, which causes the release or movement of Na^+ ions within the sample (Gili & Olegario, 2020). It included a significant quantity of exchangeable Na^+, which was the reason the improvement in fast adsorption was extremely obvious within 30 min.

3.3 Adsorption kinetics

The kinetics of MB adsorption were investigated at a temperature of 30ºC. Because kinetics may explain the adsorption mechanism and rate, all experiments were conducted at a constant temperature. The pseudo-first-order and pseudo second-order kinetic models for the MB adsorption process on DE and modified DE are illustrated in Figures 9a and b, respectively. The linear representations of both models are as follows:

$$\ln\left(q_e - q_t\right) = \ln q_e - k_1 t \quad (3)$$

$$\frac{t}{q_t} = \frac{1}{k_2 q_e^2} + \frac{t}{q_e} \quad (4)$$

Where q_e and q_t are the adsorption amounts of MB (mg/g) at equilibrium and time (min), respectively, C is a constant (mg/g) and k_1(1/min), k_2 (g/mg.min) and k_{diff} (mg/g.$t^{0.5}$) are the rate constants of the pseudo-first-order, pseudo-second-order adsorption and intraparticle diffusion, respectively.

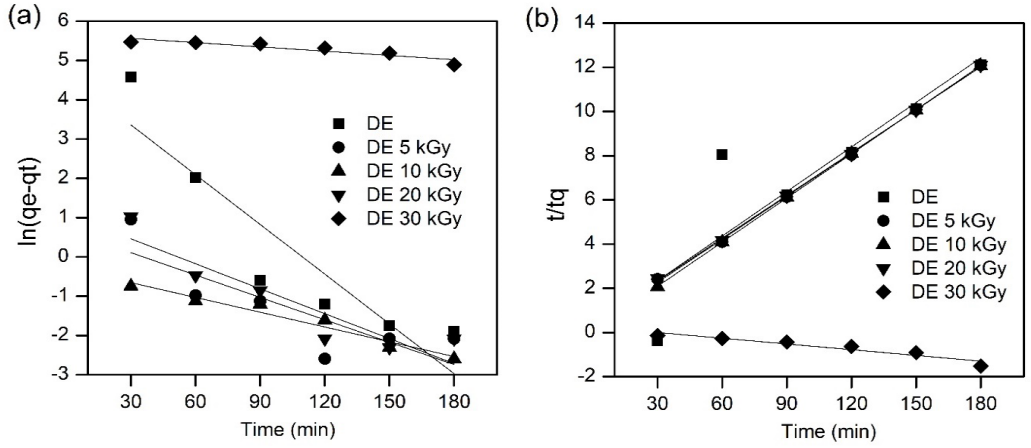

Figure 9. Kinetic model for adsorption of MB by DE and modified DE amount (a) pseudo-first order and (b) pseudo-second order

The constants generated from linear and non-linear models for pseudo-first-order and pseudo-second-order kinetics are summarized in Table 3. The kinetics of MB adsorption onto DE were analyzed using a pseudo-first-order kinetic model. It was found that the adsorption of MB onto the adsorbents was less favorable due to the disagreement between the calculated value and the experimental data. The pseudo-second-order kinetic model demonstrated the strongest correlation coefficient value (R^2 = 0.9999) for DE 10 kGy, utilizing a linear form that more effectively described the mechanism of the interactions involved in the adsorption process for MB. Furthermore, this kinetic model suggests that a chemisorption mechanism controlled the dye adsorption process. Figure 8 demonstrates a comparison between pseudo-first and pseudo-second order kinetic models for the adsorption of MB onto DE at different gamma irradiation doses (0, 5, 10, 20, 30

Table 3. Comparison of pseudo-first and pseudo-second orders, calculated and experimental (q_e), adsorption rate constants and intraparticle diffusion for adsorption of MB by modified DE

Sample	q_e(exp)	Pseudo-first Order Model			Pseudo-second Orders		
		q_e(cal)	k_1	R^2	q_e(cal)	k_2	R^2
DE	14.85	102.03	-0.0002	0.8020	14.88	0.013	0.7127
DE 5 kGy	14.875	1.96	-0.0001	0.6264	15.38	0.013	0.9990
DE 10 kGy	14.925	0.75	-0.0001	0.9461	15.02	0.046	0.9999
DE 20 kGy	14.875	2.98	-0.0001	0.8106	15.48	0.010	0.9992
DE 30 kGy	0	0	0	0.8928	0	0.0003	0.8890

kGy). The results indicate that the pseudo-second order model is the most suitable for modeling the adsorption of MB onto DE. The pseudo-second-order kinetic model provides a better fit to the experimental data compared to the pseudo-first-order model, indicating that the adsorption of MB onto DE followed a chemisorption mechanism. These findings indicate that the most significant factor that determines the rate of the adsorption process is the formation of chemical bonds between the dye molecules and the surface of DE sample.

4. Conclusions

In the present study, diatomaceous earth modified by gamma irradiation was used for MB adsorption from model textile wastewater. The results were compared to the natural diatomaceous earth. Under optimum conditions, the results confirmed that the DE 10 kGy was a suitable adsorbent with a higher percentage of MB removal (97%) within 30 min compared to the untreated irradiation sample (0% of MB removal). Equilibrium of the optimally modified DE was reached after a contact time of 30 min. The adsorption kinetics of MB molecules onto DE were accurately described using a pseudo-second-order kinetic model. The comparison of surface morphology through FE-SEM and the material structure indicated that gamma irradiation had no significant effect on the modified diatomaceous earth samples. However, irradiating an appropriate dose of γ-rays onto the surface of the DE sample created a large number of Na^+ ions, allowing for improved adsorption rate. This suggests that low dose γ-irradiation on DE could increase its maximum adsorption capability and adsorption rate, making it a cost-effective and environmentally friendly method for treating textile-polluted wastewater.

5. Acknowledgements

The authors would like to thank the Thailand Institute of Nuclear Technology (Public Organization) for the useful suggestions and provision of the instruments. This research was funded by the Thailand Science Research and Innovation (Fundamental Fund, grant number 204541).

6. Conflicts of Interest

The authors declare that they have no conflicts of interest.

References

Akafu, T., Chimdi, A., & Gomoro, K. (2019). Removal of fluoride from drinking water by sorption using diatomite modified with aluminum hydroxide. *Journal of Analytical Methods in Chemistry*, 2019, Article 4831926. https://doi.org/10.1155/2019/4831926

Albadarin, A. B., Collins, M. N., Naushad, M., Shirazian, S., Walker, G., & Mangwandi, C. (2017). Activated lignin-chitosan extruded blends for efficient adsorption of methylene blue. *Chemical Engineering Journal,* 307, 264-272. https://doi.org/10.1016/j.cej.2016.08.089

Alkan, S., Çalişkan, M., Irende, I., & Kul, A. R. (2018). Adsorption equilibrium and thermodynamics of diatomite (Çaldiran/Van) on some textile dyes. *Journal of the Chemical Society of Pakistan,* 40(3), 457-466.

Bakhsh, A. A. (2021). Gamma-ray modified polymer/clay composites: synthesis, characterization, and formulation optimization using multivariate calculus and graph theory. *Energies,* 14(9), Article 2724. https://doi.org/10.3390/en14092724

Bessedik, M., Belkebir, L., & Mansour, B. (2002). Révision de l'âge Miocène inférieur (au sensdes anciens auteurs) des dépôts du bassin du bas Chelif (Oran, Algérie): conséquences biostratigraphique et géodynamique. *Mémoires du Service géologique de l'Algérie,* 11, 167-186.

Crini, G., Lichtfouse, E., Wilson, L. D., & Morin-Crini, N. (2019). Conventional and non-conventional adsorbents for wastewater treatment. *Environmental Chemistry Letters,* 17(1), 195-213. https://doi.org/10.1007/s10311-018-0786-8

Daniels, E., & Puri, M. (1986). Physico-chemical investigations of gamma-irradiated zeolite-4A. *International Journal of Radiation Applications and Instrumentation. Part C. Radiation Physics and Chemistry,* 27(3), 225-227. https://doi.org/10.1016/1359-0197(86)90057-3

Galzerano, B., Cabello, C. I., Muñoz, M., Buonocore, G. G., Aprea, P., Liguori, B., & Verdolotti, L. (2020). Fabrication of green diatomite/chitosan-based hybrid foams with dye sorption capacity. *Materials,* 13(17), Article 3760. https://doi.org/10.3390/ma13173760

Gili, M. B. Z., & Olegario, E. M. (2020). Effects of γ-irradiation on the Cu^{2+} sorption behaviour of NaOH-modified Philippine natural zeolites. *Clay Minerals,* 55(3), 248-255. https://doi.org/10.1180/clm.2020.34

He, Y., Jiang, D. B., Jiang, D. Y., Chen, J., & Zhang, Y. X. (2018). Evaluation of MnO_2-templated iron oxide-coated diatomites for their catalytic performance in heterogeneous photo Fenton-like system. *Journal of Hazardous Materials,* 344, 230-240. https://doi.org/10.1016/j.jhazmat.2017.10.018

Holkar, C. R., Jadhav, A. J., Pinjari, D. V., Mahamuni, N. M., & Pandit, A. B. (2016). A critical review on textile wastewater treatments: Possible approaches. *Journal of Environmental Management,* 182, 351-366. https://doi.org/10.1016/j.jenvman.2016.07.090

Hsiao, Y.-H., Wang, B., La Plante, E. C., Pignatelli, I., Krishnan, N. M. A., Le Pape, Y., Neithalath, N., Bauchy, M. & Sant, G. (2019). The effect of irradiation on the atomic structure and chemical durability of calcite and dolomite. *npj Mater Degradation,* 3, Article 36. https://doi.org/10.1038/s41529-019-0098-x

Inchaurrondo, N., Font, J., Ramos, C., & Haure, P. (2016). Natural diatomites: Efficient green catalyst for Fenton-like oxidation of orange II. *Applied Catalysis B: Environmental,* 181, 481-494. https://doi.org/10.1016/j.apcatb.2015.08.022

Jia, Y., Han, W., Xiong, G. & Yang, W. (2008). Diatomite as high performance and environmental friendly catalysts for phenol hydroxylation with H_2O_2. *Science and Technology of Advanced Materials*, 8(1-2), 106-109. https://doi.org/10.1016/j.stam.2006.10.003

Kant, R. (2012). Textile dyeing industry an environmental hazard*. Natural Science,* 4(1), 22-26. https://doi.org/10.4236/ns.2012.41004

Khraisheh, M., Aldegs, Y., & Mcminn, W. (2004). Remediation of wastewater containing heavy metals using raw and modified diatomite. *Chemical Engineering Journal,* 99(2), 177-184. https://doi.org/10.1016/j.cej.2003.11.029

Lakshmi, V., Fayne, J., & Bolten, J. (2018). A comparative study of available water in the major river basins of the world. *Journal of Hydrology*, 567, 510-532. https://doi.org/10.1016/j.jhydrol.2018.10.038

Ma, T., Wu, Y., Liu, N., & Wu, Y. (2020). Hydrolyzed polyacrylamide modified diatomite waste as a novel adsorbent for organic dye removal: Adsorption performance and mechanism studies. *Polyhedron,* 175, Article 114227. https://doi.org/10.1016/j.poly.2019.114227

Memon, S., Kim, Y., Soomro, S., Soomro, M. I., & Kim, W. (2020). A new approach for freshwater production and energy recovery from an oil field. *Journal of Water Process Engineering*, 34, Article 101145. https://doi.org/10.1016/j.jwpe.2020.101145

Mohamed, E. A., Selim, A. Q., Zayed, A. M., Komarneni, S., Mobarak, M., & Seliem, M. K. (2019). Enhancing adsorption capacity of Egyptian diatomaceous earth by thermo-chemical purification: Methylene blue uptake*. Journal of Colloid and Interface Science*, 534, 408-419. https://doi.org/10.1016/j.jcis.2018.09.024

Mohseni-Bandpi, A., Al-Musawi, T. J., Ghahramani, E., Zarrabi, M., Mohebi, S., & Vahed, S. A. (2016). Improvement of zeolite adsorption capacity for cephalexin by coating with magnetic Fe_3O_4 nanoparticles. *Journal of Molecular Liquids,* 218, 615-624. https://doi.org/10.1016/j.molliq.2016.02.092

Nagaraju, A., Thejaswi, A., & Sreedhar, Y. (2016). Assessment of groundwater quality of Udayagiri area, Nellore district, Andhra Pradesh, South India using multivariate statistical techniques. *Earth Sciences Research Journal*, 20(4), E1-E7. https://doi.org/10.15446/esrj.v20n4.54555

Pathania, D., Sharma, S., & Singh, P. (2017). Removal of methylene blue by adsorption onto activated carbon developed from *Ficus carica* bast. *Arabian Journal of Chemistry,* 10, S1445-S1451. https://doi.org/10.1016/j.arabjc.2013.04.021

Rautiyal, P., Gupta, G., Edge, R., Leay, L., Daubney, A., Patel, M. K., Jones, A. H. & Bingham, P. A. (2021). Gamma irradiation-induced defects in borosilicate glasses for high-level radioactive waste immobilisation. *Journal of Nuclear Materials*, 544, Article 152702. https://doi.org/10.1016/j.jnucmat.2020.152702

Rizqi, H. D., & Purnomo, A. S. (2017). The ability of brown-rot fungus *Daedalea dickinsii* to decolorize and transform methylene blue dye. *World Journal of Microbiology and Biotechnology,* 33(5), Article 92. https://doi.org/10.1007/s11274-017-2256-z

Robinson, T., McMullan, G., Marchant, R., & Nigam, P. (2001). Remediation of dyes in textile effluent: A critical review on current treatment technologies with a proposed alternative. *Bioresource Technology,* 77(3), 247-255. https://doi.org/10.1016/s0960-8524(00)00080-8

Rytwo, G., Tropp, D., & Serban, C. (2002). Adsorption of diquat, paraquat and methyl green on sepiolite: Experimental results and model calculations. *Applied Clay Science*, 20(6), 273-282. https://doi.org/10.1016/s0169-1317(01)00068-0

Salman, T., Temel, F. A., Turan, N. G., & Ardali, Y. (2016). Adsorption of lead (II) ions onto diatomite from aqueous solutions: Mechanism, isotherm and kinetic studies. *Global NEST Journal,* 18(1), 1-10. https://doi.org/10.30955/gnj.001564

Spinks, J. W. T., & Woods, K. J. (1990). *Introduction of radiation chemistry*. 3rd Edition, John Wiley & Sons.

Thamaraiselvan, C., & Noel, M. (2015). Membrane processes for dye wastewater treatment: Recent progress in fouling control. *Critical Reviews in Environmental Science and Technology,* 45(10), 1007-1040. https://doi.org/10.1080/10643389.2014.900242

Touina, A., Chernai, S., Mansour, B., Hadjar, H., Ouakouak, A., & Hamdi, B. (2021). Characterization and efficient dye discoloration of Algerian diatomite from Ouled Djilali-Mostaganem. *SN Applied Sciences*, 3(4), Article 476. https://doi.org/10.1007/s42452-021-04334-9

Vassileva, P., Gentscheva, G., Ivanova, E., Tzvetkova, P., Voykova, D., & Apostolova, M. (2011). Characterization of natural diatomites from Bulgaria. *Comptes Rendus de l'Académie Bulgare des Sciences,* 64(6), 823-830.

Wang, M., Zhang, K., Wu, M., Wu, Q., Liu, J., Yang, J., & Zhang, J. (2019). Unexpectedly high adsorption capacity of esterified hydroxyapatite for heavy metal removal. *Langmuir*, 35(49), 16111-16119. https://doi.org/10.1021/acs.langmuir.9b02373

Yu, Z.-H., Zhang, Y.-F., Zhai, S.-R., Wang, Y., Pan, Y.-Z., & Meng, C.-G. (2015). Amino-modified mesoporous sorbents for efficient Cd(II) adsorption prepared using non-chemical diatomite as precursor. *Journal of Sol-Gel Science and Technology,* 78(1), 110-119. https://doi.org/10.1007/s10971-015-3933-8